

# Rigid Body Pose Estimation based on the Lagrange-d'Alembert Principle<sup>\*</sup>

Maziar Izadi <sup>a</sup>, Amit K. Sanyal <sup>b</sup>,

<sup>a</sup>*Department of Mechanical and Aerospace Engineering, New Mexico State University, Las Cruces, NM 88003 USA.*

<sup>b</sup>*Department of Mechanical and Aerospace Engineering, Syracuse University, Syracuse, NY 13244 USA (previously with New Mexico State University).*

---

## Abstract

Stable estimation of rigid body pose and velocities from noisy measurements, without any knowledge of the dynamics model, is treated using the Lagrange-d'Alembert principle from variational mechanics. With body-fixed optical and inertial sensor measurements, a Lagrangian is obtained as the difference between a kinetic energy-like term that is quadratic in velocity estimation error and the sum of two artificial potential functions; one obtained from a generalization of Wahba's function for attitude estimation and another which is quadratic in the position estimate error. An additional dissipation term that is linear in the velocity estimation error is introduced, and the Lagrange-d'Alembert principle is applied to the Lagrangian with this dissipation. A Lyapunov analysis shows that the state estimation scheme so obtained provides stable asymptotic convergence of state estimates to actual states in the absence of measurement noise, with an almost global domain of attraction. This estimation scheme is discretized for computer implementation using discrete variational mechanics, as a first order Lie group variational integrator. The continuous and discrete pose estimation schemes require optical measurements of at least three inertially fixed landmarks or beacons in order to estimate instantaneous pose. The discrete estimation scheme can also estimate velocities from such optical measurements. Moreover, all states can be estimated during time periods when measurements of only two inertial vectors, the angular velocity vector, and one feature point position vector are available in body frame. In the presence of bounded measurement noise in the vector measurements, numerical simulations show that the estimated states converge to a bounded neighborhood of the actual states.

---

## 1 Introduction

Estimation of rigid body translational and rotational motion is indispensable for operations of spacecraft, unmanned aerial and underwater vehicles. Autonomous state estimation of a rigid body based on inertial vector measurement and visual feedback from stationary landmarks, in the absence of a dynamics model for the rigid body, is analyzed here. The estimation scheme proposed here can also be applied to *relative state* estimation with respect to moving objects [25]. This estimation scheme can enhance the autonomy and reliability of unmanned vehicles in uncertain GPS-denied environments. Salient features of this estimation scheme are: (1) use of onboard optical and inertial sensors, with or without rate gyros, for autonomous navigation; (2) robustness to uncertainties and lack of knowledge of dynamics; (3) low computational complexity for easy implementation with

onboard processors; (4) proven stability with large domain of attraction for state estimation errors; and (5) versatile enough to estimate motion with respect to stationary as well as moving objects. Robust state estimation of rigid bodies in the absence of complete knowledge of their dynamics, is required for their safe, reliable, and autonomous operations in poorly known conditions. In practice, the dynamics of a vehicle may not be perfectly known, especially when the vehicle is under the action of poorly known forces and moments. The scheme proposed here has a single, stable algorithm for the coupled translational and rotational motion of rigid bodies using onboard optical (which may include infra-red) and inertial sensors. This avoids the need for measurements from external sources, like GPS, which may not be available in indoor, underwater or cluttered environments [2, 17, 23].

Attitude estimators using unit quaternions for attitude representation may be *unstable in the sense of Lyapunov*, unless they identify antipodal quaternions with a single attitude. This is also the case for attitude control schemes based on continuous feedback of unit quaternions, as shown in [3, 7, 28]. One adverse consequence

---

<sup>\*</sup> This paper was not presented at any IFAC meeting. Corresponding author A. K. Sanyal. Tel. +1(575) 646-2580.

*Email addresses:* [mi@nmsu.edu](mailto:mi@nmsu.edu) (Maziar Izadi), [aksanyal@syr.edu](mailto:aksanyal@syr.edu) (Amit K. Sanyal).

of these unstable estimation and control schemes is that they end up taking longer to converge compared with stable schemes under similar initial conditions and initial transient behavior. Continuous-time attitude observers and filtering schemes on  $SO(3)$  and  $SE(3)$  have been reported in, e.g., [6, 14, 15, 18, 19, 20, 27, 30, 36, 37]. These estimators do not suffer from kinematic singularities like estimators using coordinate descriptions of attitude, and they do not suffer from unwinding as they do not use unit quaternions. The maximum-likelihood (minimum energy) filtering method of Mortensen [26] was recently applied to attitude estimation, resulting in a nonlinear attitude estimation scheme that seeks to minimize the stored “energy” in measurement errors [1, 39, 40]. This scheme is obtained by applying Hamilton-Jacobi-Bellman (HJB) theory [16] to the state space of attitude motion [39]. Since the HJB equation can only be approximately solved with increasingly unwieldy expressions for higher order approximations, the resulting filter is only “near optimal” up to second order. Unlike filtering schemes that are based on approximate or “near optimal” solutions of the HJB equation and do not have provable stability, the estimation scheme obtained here can be solved exactly, and is shown to be almost globally asymptotically stable. Moreover, unlike filters based on Kalman filtering, the estimator proposed here does not presume any knowledge of the statistics of the initial state estimate or the sensor noise. Indeed, for vector measurements using optical sensors with limited field-of-view, the probability distribution of measurement noise needs to have compact support, unlike standard Gaussian noise processes that are commonly used to describe such noisy measurements.

The variational attitude estimator recently appeared in [10, 11, 12], where it was shown to be almost globally asymptotically stable. Some of the advantages of this scheme over some commonly used competing schemes are reported in [9]. This paper is the variational estimation framework to coupled rotational (attitude) and translational motion, as exhibited by maneuvering vehicles like UAVs. In such applications, designing separate state estimators for the translational and rotational motions may not be effective and may lead to poor navigation. For navigation and tracking the motion of such vehicles, the approach proposed here for robust and stable estimation of the coupled translational and rotational motion will be more effective than de-coupled estimation of translational and rotational motion states. Moreover, like other vision-inertial navigation schemes [33, 34], the estimation scheme proposed here does not rely on GPS. However, unlike many other vision-inertial estimation schemes, the estimation scheme proposed here can be implemented without any direct velocity measurements. Since rate gyros are usually corrupted by high noise content and bias [8], such a velocity measurement-free scheme can result in fault tolerance in the case of faults with rate gyros. Additionally, this estimation scheme can be extended to relative pose estimation between vehicles

from optical measurements, without direct communications or measurements of relative velocities.

The contents of this article are organized as follows. In Section 2, the problem of motion estimation of a rigid body using onboard optical and inertial sensors is introduced. The measurement model is introduced and rigid body states are related to these measurements. Section 3 introduces artificial energy terms representing the measurement residuals corresponding to the rigid body state estimates. The Lagrange-d’Alembert principle is applied to the Lagrangian constructed from these energy terms with a Rayleigh dissipation term linear in the velocity measurement residual, to give the continuous time state estimator. Particular versions of this estimation scheme are provided for the cases when direct velocity measurements are not available and when only angular velocity is directly measured. Section 4 proves the stability of the resulting variational estimator. It is shown that, in the absence of measurement noise, state estimates converge to actual states asymptotically and the domain of attraction is an open dense subset of the state space. In Section 5, the variational pose estimator is discretized as a Lie group variational integrator, by applying the discrete Lagrange-d’Alembert principle to discretizations of the Lagrangian and the dissipation term. This estimator is simulated numerically in Section 6, for two cases: the case where at least three beacons are measured at each time instant; and the under-determined case, where occasionally less than three beacons are observed. For these simulations, true states of an aerial vehicle are generated using a given dynamics model. Optical/inertial measurements are generated, assuming bounded noise in sensor readings. Using these measurements, state estimates are shown to converge to a neighborhood of actual states, for both cases simulated. Finally, Section 7 lists the contributions and possible future extensions of the work presented in this paper.

## 2 Navigation using Optical and Inertial Sensors

Consider a vehicle in spatial (rotational and translational) motion. Onboard estimation of the pose of the vehicle involves assigning a coordinate frame fixed to the vehicle body, and another coordinate frame fixed in the environment which takes the role of the inertial frame. Let  $O$  denote the observed environment and  $S$  denote the vehicle. Let  $\mathcal{S}$  denote a coordinate frame fixed to  $S$  and  $\mathcal{O}$  be a coordinate frame fixed to  $O$ , as shown in Fig. 1. Let  $R \in SO(3)$  denote the rotation matrix from frame  $\mathcal{S}$  to frame  $\mathcal{O}$  and  $b$  denote the position of origin of  $\mathcal{S}$  expressed in frame  $\mathcal{O}$ . The pose (transformation) from body fixed frame  $\mathcal{S}$  to inertial frame  $\mathcal{O}$  is then given by

$$\mathbf{g} = \begin{bmatrix} R & b \\ 0 & 1 \end{bmatrix} \in SE(3). \quad (1)$$

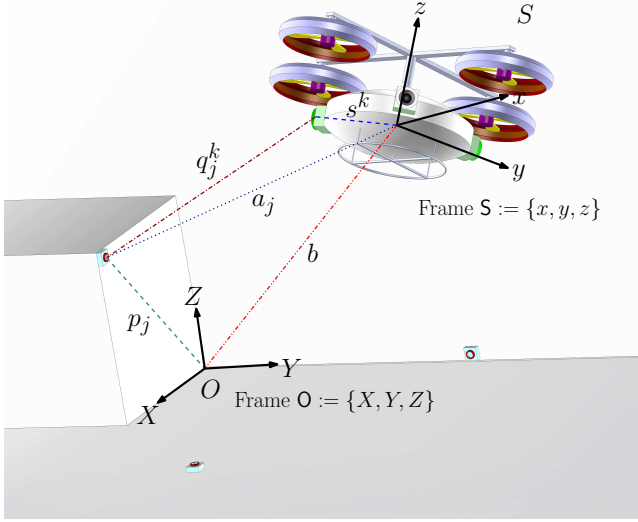


Fig. 1. Inertial landmarks on  $O$  as observed from vehicle  $S$  with optical measurements.

Consider vectors known in inertial frame  $O$  measured by inertial sensors in the vehicle-fixed frame  $S$ ; let  $\beta$  be the number of such vectors. In addition, consider position vectors of a few stationary points in the inertial frame  $O$  measured by optical (vision or lidar) sensors in the vehicle-fixed frame  $S$ . Velocities of the vehicle may be directly measured or can be estimated by linear filtering of the optical position vector measurements [12]. Assume that these optical measurements are available for  $j$  points at time  $t$ , whose positions are known in frame  $O$  as  $p_j$ ,  $j \in \mathcal{I}(t)$ , where  $\mathcal{I}(t)$  denotes the index set of beacons observed at time  $t$ . Note that the observed stationary beacons or landmarks may vary over time due to the vehicle's motion. These points generate  $\binom{j}{2}$  unique relative position vectors, which are the vectors connecting any two of these landmarks. When two or more position vectors are optically measured, the number of vector measurements that can be used to estimate attitude is  $\binom{j}{2} + \beta$ . This number needs to be at least two (i.e.,  $\binom{j}{2} + \beta \geq 2$ ) at an instant, for the attitude to be uniquely determined at that instant. In other words, if at least two inertial vectors are measured at all instants (i.e.,  $\beta \geq 2$ ), then beacon position measurements are not required for estimating attitude. However, at least one beacon or feature point position measurement is still required to estimate the position of the vehicle. Note that the use of two vector measurements for attitude determination was first proposed by the TRIAD algorithm in the 1960s [4].

### 2.1 Pose Measurement Model

Denote the position of an optical sensor and the unit vector from that sensor to an observed beacon in frame  $S$  as  $s^k \in \mathbb{R}^3$  and  $u^k \in \mathbb{S}^2$ ,  $k = 1, \dots, \kappa$ , respectively. Denote the relative position of the  $j^{\text{th}}$  stationary beacon observed by the  $k^{\text{th}}$  sensor expressed in frame  $S$  as  $q_j^k$ .

Thus, in the absence of measurement noise

$$p_j = R(q_j^k + s^k) + b = Ra_j + b, \quad j \in \mathcal{I}(t), \quad (2)$$

where  $a_j = q_j^k + s^k$ , are positions of these points expressed in  $S$ . In practice, the  $a_j$  are obtained from range measurements that have additive noise; we denote as  $a_j^m$  the measured vectors. In the case of lidar range measurements, these are given by

$$a_j^m = (q_j^k)^m + s^k = (\varrho_j^k)^m u^k + s^k, \quad j \in \mathcal{I}(t), \quad (3)$$

where  $(\varrho_j^k)^m$  is the measured range to the point by the  $k^{\text{th}}$  sensor. The mean of the vectors  $p_j$  and  $a_j^m$  are denoted as  $\bar{p}$  and  $\bar{a}^m$  respectively, and satisfy

$$\bar{a}^m = R^T(\bar{p} - b) + \bar{\varsigma}, \quad (4)$$

where  $\bar{p} = \frac{1}{j} \sum_{j=1}^j p_j$ ,  $\bar{a}^m = \frac{1}{j} \sum_{j=1}^j a_j^m$  and  $\bar{\varsigma}$  is the additive measurement noise obtained by averaging the measurement noise vectors for each of the  $a_j$ . Consider the  $\binom{j}{2}$  relative position vectors from optical measurements, denoted as  $d_j = p_\lambda - p_\ell$  in frame  $O$  and the corresponding vectors in frame  $S$  as  $l_j = a_\lambda - a_\ell$ , for  $\lambda, \ell \in \mathcal{I}(t)$ ,  $\lambda \neq \ell$ . The  $\beta$  measured inertial vectors are included in the set of  $d_j$ , and their corresponding measured values expressed in frame  $S$  are included in the set of  $l_j$ . If the total number of measured vectors (both optical and inertial),  $\binom{j}{2} + \beta = 2$ , then  $l_3 = l_1 \times l_2$  is considered a third measured direction in frame  $S$  with corresponding vector  $d_3 = d_1 \times d_2$  in frame  $O$ . Therefore,

$$d_j = Rl_j \Rightarrow D = RL, \quad (5)$$

where  $D = [d_1 \ \dots \ d_n]$ ,  $L = [l_1 \ \dots \ l_n] \in \mathbb{R}^{3 \times n}$  with  $n = 3$  if  $\binom{j}{2} + \beta = 2$  and  $n = \binom{j}{2} + \beta$  if  $\binom{j}{2} + \beta > 2$ . Note that the matrix  $D$  consists of vectors known in frame  $O$ . Denote the measured value of matrix  $L$  in the presence of measurement noise as  $L^m$ . Then,

$$L^m = R^T D + \mathcal{L}, \quad (6)$$

where  $\mathcal{L} \in \mathbb{R}^{3 \times n}$  consists of the additive noise in the vector measurements made in the body frame  $S$ .

### 2.2 Velocities Measurement Model

Denote the angular and translational velocity of the rigid body expressed in body fixed frame  $S$  by  $\Omega$  and  $\nu$ , respectively. Therefore, one can write the kinematics of the rigid body as

$$\dot{\Omega} = R\Omega^\times, \dot{b} = R\nu \Rightarrow \dot{g} = g\xi^\vee, \quad (7)$$

where  $\xi = \begin{bmatrix} \Omega \\ \nu \end{bmatrix} \in \mathbb{R}^6$  and  $\xi^\vee = \begin{bmatrix} \Omega^\times & \nu \\ 0 & 0 \end{bmatrix}$  and  $(\cdot)^\times : \mathbb{R}^3 \rightarrow$

$\mathfrak{so}(3) \subset \mathbb{R}^{3 \times 3}$  is the skew-symmetric cross-product operator that gives the vector space isomorphism between  $\mathbb{R}^3$  and  $\mathfrak{so}(3)$ :

$$\chi^\times = \begin{bmatrix} \chi_1 \\ \chi_2 \\ \chi_3 \end{bmatrix}^\times = \begin{bmatrix} 0 & -\chi_3 & \chi_2 \\ \chi_3 & 0 & -\chi_1 \\ -\chi_2 & \chi_1 & 0 \end{bmatrix}. \quad (8)$$

For the general development of the motion estimation scheme, it is assumed that the velocities are directly measured. The estimator is then extended to cover the cases where: (i) only angular velocity is directly measured; and (ii) none of the velocities are directly measured.

### 3 Dynamic Estimation of Motion from Proximity Measurements

In order to obtain state estimation schemes from measurements as outlined in Section 2 in continuous time, the Lagrange-d'Alembert principle is applied to an action functional of a Lagrangian of the state estimate errors, with a dissipation term linear in the velocities estimate error. This section presents the estimation scheme obtained using this approach. Denote the estimated pose and its kinematics as

$$\hat{\mathbf{g}} = \begin{bmatrix} \hat{R} & \hat{b} \\ 0 & 1 \end{bmatrix} \in \text{SE}(3), \quad \dot{\hat{\mathbf{g}}} = \hat{\mathbf{g}} \hat{\xi}^\vee, \quad (9)$$

where  $\hat{\xi}$  is rigid body velocities estimate, with  $\hat{\mathbf{g}}_0$  as the initial pose estimate and the pose estimation error as

$$\mathbf{h} = \mathbf{g} \hat{\mathbf{g}}^{-1} = \begin{bmatrix} Q & b - Q\hat{b} \\ 0 & 1 \end{bmatrix} = \begin{bmatrix} Q & x \\ 0 & 1 \end{bmatrix} \in \text{SE}(3), \quad (10)$$

where  $Q = R\hat{R}^\text{T}$  is the attitude estimation error and  $x = b - Q\hat{b}$ . Then one obtains, in the case of perfect measurements,

$$\dot{\mathbf{h}} = \mathbf{h} \varphi^\vee, \quad \text{where } \varphi(\hat{\mathbf{g}}, \xi^m, \hat{\xi}) = \begin{bmatrix} \omega \\ v \end{bmatrix} = \text{Ad}_{\hat{\mathbf{g}}}(\xi^m - \hat{\xi}), \quad (11)$$

where  $\text{Ad}_g = \begin{bmatrix} \mathcal{R} & 0 \\ \hat{b}^\times \mathcal{R} & \mathcal{R} \end{bmatrix}$  for  $g = \begin{bmatrix} \mathcal{R} & \hat{b} \\ 0 & 1 \end{bmatrix}$ . The attitude and position estimation error dynamics are also in the form

$$\dot{Q} = Q\omega^\times, \quad \dot{x} = Qv. \quad (12)$$

#### 3.1 Lagrangian from Measurement Residuals

Consider the sum of rotational and translational measurement residuals between the measurements and estimated pose as a potential energy-like function. Defining the trace inner product on  $\mathbb{R}^{n_1 \times n_2}$  as

$$\langle A_1, A_2 \rangle := \text{trace}(A_1^\text{T} A_2), \quad (13)$$

the rotational potential function (Wahba's cost function [38]) is expressed as

$$\mathcal{U}_r^0(\hat{\mathbf{g}}, L^m, D) = \frac{1}{2} \langle D - \hat{R}L^m, (D - \hat{R}L^m)W \rangle, \quad (14)$$

where  $W = \text{diag}(w_j) \in \mathbb{R}^{n \times n}$  is a positive diagonal matrix of weight factors for the measured  $l_j^m$ . Consider the translational potential function

$$\mathcal{U}_t(\hat{\mathbf{g}}, \bar{a}^m, \bar{p}) = \frac{1}{2} \kappa y^\text{T} y = \frac{1}{2} \kappa \|\bar{p} - \hat{R}\bar{a}^m - \hat{b}\|^2, \quad (15)$$

where  $\bar{p}$  is defined by (4),  $y \equiv y(\hat{\mathbf{g}}, \bar{a}^m, \bar{p}) = \bar{p} - \hat{R}\bar{a}^m - \hat{b}$  and  $\kappa$  is a positive scalar. Therefore, the total potential function is defined as the sum of the generalization of (14) defined in [10, 29] for attitude determination on  $\text{SO}(3)$ , and the translational energy (15) as

$$\begin{aligned} \mathcal{U}(\hat{\mathbf{g}}, L^m, D, \bar{a}^m, \bar{p}) &= \mathcal{U}_r(\hat{\mathbf{g}}, L^m, D) + \mathcal{U}_t(\hat{\mathbf{g}}, \bar{a}^m, \bar{p}) \\ &= \Phi(\mathcal{U}_r^0(\hat{\mathbf{g}}, L^m, D)) + \mathcal{U}_t(\hat{\mathbf{g}}, \bar{a}^m, \bar{p}) \\ &= \Phi\left(\frac{1}{2} \langle D - \hat{R}L^m, (D - \hat{R}L^m)W \rangle\right) \\ &\quad + \frac{1}{2} \kappa \|\bar{p} - \hat{R}\bar{a}^m - \hat{b}\|^2, \end{aligned} \quad (16)$$

where  $W$  is positive definite (not necessarily diagonal), and  $\Phi : [0, \infty) \mapsto [0, \infty)$  is a  $\mathcal{C}^2$  function that satisfies  $\Phi(0) = 0$  and  $\Phi'(\chi) > 0$  for all  $\chi \in [0, \infty)$ . Furthermore,  $\Phi'(\cdot) \leq \alpha(\cdot)$  where  $\alpha(\cdot)$  is a Class- $\mathcal{K}$  function [13] and  $\Phi'(\cdot)$  denotes the derivative of  $\Phi(\cdot)$  with respect to its argument. Because of these properties of the function  $\Phi$ , the critical points and their indices coincide for  $\mathcal{U}_r^0$  and  $\mathcal{U}_r$  [10]. Define the kinetic energy-like function:

$$\mathcal{T}(\varphi(\hat{\mathbf{g}}, \xi^m, \hat{\xi})) = \frac{1}{2} \varphi(\hat{\mathbf{g}}, \xi^m, \hat{\xi})^\text{T} \mathbb{J} \varphi(\hat{\mathbf{g}}, \xi^m, \hat{\xi}), \quad (17)$$

where  $\mathbb{J} \in \mathbb{R}^{6 \times 6} > 0$  is an artificial inertia-like kernel matrix. Note that in contrast to rigid body inertia matrix,  $\mathbb{J}$  is not subject to intrinsic physical constraints like the triangle inequality, which dictates that the sum of any two eigenvalues of the inertia matrix has to be larger than the third. Instead,  $\mathbb{J}$  is a gain matrix that can be used to tune the estimator. For notational convenience,  $\varphi(\hat{\mathbf{g}}, \xi^m, \hat{\xi})$  is denoted as  $\varphi$  from now on; this quantity

is the velocities estimation error in the absence of measurement noise. Now define the Lagrangian

$$\mathcal{L}(\hat{\mathbf{g}}, L^m, D, \bar{a}^m, \bar{p}, \varphi) = \mathcal{T}(\varphi) - \mathcal{U}(\hat{\mathbf{g}}, L^m, D, \bar{a}^m, \bar{p}), \quad (18)$$

and the corresponding action functional over an arbitrary time interval  $[t_0, T]$  for  $T > 0$ ,

$$S(\mathcal{L}(\hat{\mathbf{g}}, L^m, D, \bar{a}^m, \bar{p}, \varphi)) = \int_{t_0}^T \mathcal{L}(\hat{\mathbf{g}}, L^m, D, \bar{a}^m, \bar{p}, \varphi) dt, \quad (19)$$

such that  $\dot{\hat{\mathbf{g}}} = \hat{\mathbf{g}}(\hat{\xi})^\vee$ . The following statement gives the form of the Lagrangian when perfect (noise-free) measurements are available, and derives the variational estimator for rigid body pose and velocities.

**Lemma 3.1** *In the absence of measurement noise, the Lagrangian is of the form*

$$\mathcal{L}(\mathbf{h}, D, \bar{p}, \varphi) = \frac{1}{2} \varphi^T \mathbb{J} \varphi - \Phi(\langle I - Q, K \rangle) - \frac{1}{2} \kappa y^T y, \quad (20)$$

where  $K = DWD^T$  and  $y \equiv y(\mathbf{h}, \bar{p}) = Q^T x + (I - Q^T) \bar{p}$ .

*Proof:* Suppose that all the measured states are noise free. Therefore, one can replace  $L^m = L$ ,  $\bar{a}^m = \bar{a}$  and  $\xi^m = \xi$ . The rotational potential function (14) can be replaced by

$$\begin{aligned} \mathcal{U}_r^0(\mathbf{h}, D) &= \frac{1}{2} \langle D - \hat{R}L^m, (D - \hat{R}L^m)W \rangle \\ &= \frac{1}{2} \langle D - Q^T D, (D - Q^T D)W \rangle \\ &= \frac{1}{2} \langle I - Q^T, (I - Q^T)DWD^T \rangle = \langle I - Q, K \rangle, \end{aligned} \quad (21)$$

since  $\hat{R}E = Q^T D$  for the noise-free case. In addition,

$$\begin{aligned} y(\mathbf{h}, \bar{p}) &= \bar{p} - \hat{R}\bar{a}^m - \hat{b} = \bar{p} - \hat{R}\bar{a} - \hat{b} \\ &= \bar{p} - Q^T R\bar{a} - Q^T(b - x) = Q^T x + (I - Q^T)\bar{p}. \end{aligned} \quad (22)$$

The translational potential function in the absence of measurement noise can be expressed as

$$\mathcal{U}_t(\mathbf{h}, \bar{p}) = \frac{1}{2} \kappa y^T y. \quad (23)$$

Therefore, the total potential energy function is

$$\begin{aligned} \mathcal{U}(\mathbf{h}, D, \bar{p}) &= \mathcal{U}_r(\mathbf{h}, D) + \mathcal{U}_t(\mathbf{h}, \bar{p}) \\ &= \Phi(\mathcal{U}_r^0(\mathbf{h}, D)) + \mathcal{U}_t(\mathbf{h}, \bar{p}) \\ &= \Phi(\langle I - Q, K \rangle) + \frac{1}{2} \kappa y^T y, \end{aligned} \quad (24)$$

and the kinetic energy function is

$$\mathcal{T}(\varphi) = \frac{1}{2} \varphi^T \mathbb{J} \varphi. \quad (25)$$

Substituting (24) and (25) into:

$$\begin{aligned} \mathcal{L}(\mathbf{h}, D, \bar{p}, \varphi) &= \mathcal{T}(\varphi) - \mathcal{U}(\mathbf{h}, D, \bar{p}) \\ &= \mathcal{T}(\varphi) - \Phi(\mathcal{U}_r^0(\mathbf{h}, D)) - \mathcal{U}_t(\mathbf{h}, \bar{p}), \end{aligned} \quad (26)$$

gives the Lagrangian (20) for the noise-free case.  $\square$

As in [10], the positive definite weight matrix  $W$  can be selected according to the following lemma:

**Lemma 3.2** *Let  $\text{rank}(D) = 3$ . Let the singular value decomposition of  $D$  be given by*

$$\begin{aligned} D &:= U_D \Sigma_D V_D^T \text{ where } U_D \in \text{O}(3), V_D \in \text{O}(n), \\ \Sigma_D &\in \text{Diag}^+(3, n), \end{aligned} \quad (27)$$

and  $\text{Diag}^+(n_1, n_2)$  is the vector space of  $n_1 \times n_2$  matrices with positive entries along the main diagonal and all other components zero. Let  $\sigma_1, \sigma_2, \sigma_3$  denote the main diagonal entries of  $\Sigma_D$ . Further, let the positive definite weight matrix  $W$  be given by

$$W = V_D W_0 V_D^T \text{ where } W_0 \in \text{Diag}^+(n, n) \quad (28)$$

and the first three diagonal entries of  $W_0$  are given by

$$w_1 = \frac{\varsigma_1}{\sigma_1^2}, w_2 = \frac{\varsigma_2}{\sigma_2^2}, w_3 = \frac{\varsigma_3}{\sigma_3^2} \text{ where } \varsigma_1, \varsigma_2, \varsigma_3 > 0. \quad (29)$$

Then,  $K = DWD^T$  is positive definite and

$$K = U_D \Delta U_D^T \text{ where } \Delta = \text{diag}(\varsigma_1, \varsigma_2, \varsigma_3), \quad (30)$$

is its eigendecomposition. Moreover, if  $\varsigma_i \neq \varsigma_j$  for  $i \neq j$  and  $i, j \in \{1, 2, 3\}$ , then  $\langle I - Q, K \rangle$  is a Morse function whose critical points are

$$Q \in C_Q = \{I, Q_1, Q_2, Q_3\} \text{ where } Q_i = 2U_D I_i I_i^T U_D^T - I, \quad (31)$$

and  $I_i$  is the  $i^{\text{th}}$  column vector of the identity  $I \in \text{SO}(3)$ .

The proof is presented in [10].

### 3.2 Variational Estimator for Pose and Velocities

The nonlinear variational estimator obtained by applying the Lagrange-d'Alembert principle to the Lagrangian (18) with a dissipation term linear in the velocities estimation error, is given by the following statement.

**Theorem 3.3** *The nonlinear variational estimator for pose and velocities is given by*

$$\begin{cases} \mathbb{J}\dot{\varphi} &= \text{ad}_\varphi^* \mathbb{J}\varphi - Z(\hat{\mathbf{g}}, L^m, D, \bar{a}^m, \bar{p}) - \mathbb{D}\varphi, \\ \hat{\xi} &= \xi^m - \text{Ad}_{\hat{\mathbf{g}}^{-1}} \varphi, \\ \dot{\hat{\mathbf{g}}} &= \hat{\mathbf{g}}(\hat{\xi})^\vee, \end{cases} \quad (32)$$

where  $\text{ad}_\zeta^* = (\text{ad}_\zeta)^T$  with  $\text{ad}_\zeta$  defined by (36), and  $Z(\hat{\mathbf{g}}, L^m, D, \bar{a}^m, \bar{p})$  is defined by

$$Z(\hat{\mathbf{g}}, L^m, D, \bar{a}^m, \bar{p}) = \begin{bmatrix} \Phi'(\mathcal{U}_r^0(\hat{\mathbf{g}}, L^m, D)) S_\Gamma(\hat{R}) + \kappa \bar{p}^\times y \\ \kappa y \end{bmatrix}, \quad (33)$$

where  $\mathcal{U}_r^0(\hat{\mathbf{g}}, L^m, D)$  is defined as (14),  $y \equiv y(\hat{\mathbf{g}}, \bar{a}^m, \bar{p}) = \bar{p} - \hat{R}\bar{a}^m - \hat{\mathbf{b}}$  and

$$\begin{aligned} S_\Gamma(\hat{R}) &= \text{vex}(\Gamma \hat{R}^T - \hat{R} \Gamma^T) \\ &= \text{vex}(DW(L^m)^T \hat{R}^T - \hat{R} L^m W D^T), \end{aligned} \quad (34)$$

$\Gamma = DW(L^m)^T$  and  $\text{vex}(\cdot) : \mathfrak{so}(3) \rightarrow \mathbb{R}^3$  is the inverse of the  $(\cdot)^\times$  map.

*Proof:* A Rayleigh dissipation term linear in the velocities of the form  $\mathbb{D}\varphi$  where  $\mathbb{D} \in \mathbb{R}^{6 \times 6} > 0$  is used in addition to the Lagrangian (20), and the Lagrange-d'Alembert principle from variational mechanics is applied to obtain the estimator on TSE(3). *Reduced variations* with respect to  $\mathbf{h}$  and  $\varphi$  [5, 21] are applied, given by

$$\delta \mathbf{h} = \mathbf{h}\eta^\vee, \quad \delta \varphi = \dot{\eta} + \text{ad}_\varphi \eta, \quad (35)$$

$$\text{where } \eta^\vee = \begin{bmatrix} \Sigma^\times & \rho \\ 0 & 0 \end{bmatrix} \text{ and } \text{ad}_\zeta = \begin{bmatrix} \mathbf{w}^\times & 0 \\ \mathbf{v}^\times & \mathbf{w}^\times \end{bmatrix}, \quad (36)$$

for  $\eta = \begin{bmatrix} \Sigma \\ \rho \end{bmatrix} \in \mathbb{R}^6$  and  $\zeta = \begin{bmatrix} \mathbf{w} \\ \mathbf{v} \end{bmatrix} \in \mathbb{R}^6$ , with  $\eta(t_0) = \eta(T) = 0$ . This leads to the expression:

$$\delta_{\mathbf{h}, \varphi} \mathcal{S}(\mathcal{L}(\mathbf{h}, D, \bar{p}, \varphi)) = \int_{t_0}^T \eta^T \mathbb{D} \varphi dt. \quad (37)$$

Note that the variations of the attitude and position estimation errors are of the form

$$\delta Q = Q \Sigma^\times, \quad \delta x = Q \rho, \quad (38)$$

respectively. Applying reduced variations to the rotational potential energy term (21), one obtains

$$\begin{aligned} \delta_Q \mathcal{U}_r^0(\mathbf{h}, D) &= \langle -Q \Sigma^\times, K \rangle = \frac{1}{2} \langle \Sigma^\times, KQ - Q^T K \rangle \\ &= S_K^T(Q) \Sigma, \end{aligned} \quad (39)$$

where

$$S_K(Q) = \text{vex}(KQ - Q^T K). \quad (40)$$

Taking first variation of the translational potential energy term (23) with respect to  $Q$  and  $x$  yields:

$$\begin{aligned} \delta_{\mathbf{h}} \mathcal{U}_t(\mathbf{h}, \bar{p}) &= \kappa (\delta x + \delta Q \bar{p})^T \{x + (Q - I) \bar{p}\} \\ &= \kappa (\rho^T y + \Sigma^T \bar{p}^\times y). \end{aligned} \quad (41)$$

Therefore, the first variation of the total potential energy (24) with respect to estimation errors is

$$\delta_{\mathbf{h}} \mathcal{U}(\mathbf{h}, D, \bar{p}) = Z^T(\mathbf{h}, D, \bar{p}) \eta, \quad (42)$$

where  $Z(\mathbf{h}, D, \bar{p})$  is defined by

$$Z(\mathbf{h}, D, \bar{p}) = \begin{bmatrix} \Phi'(\langle I - Q, K \rangle) S_K(Q) + \kappa \bar{p}^\times \{Q^T x + (I - Q^T) \bar{p}\} \\ \kappa \{Q^T x + (I - Q^T) \bar{p}\} \end{bmatrix}. \quad (43)$$

Taking the first variation of the kinetic energy term (25) with respect to  $\varphi$  results in:

$$\delta_\varphi \mathcal{T}(\varphi) = \varphi^T \mathbb{J} \delta \varphi = \varphi^T \mathbb{J} (\dot{\eta} + \text{ad}_\varphi \eta), \quad (44)$$

applying the reduced variation for  $\delta \varphi$  as given in (35). Therefore, the first variation of the action functional (19) is obtained as

$$\begin{aligned} \delta_{\mathbf{h}, \varphi} \mathcal{S}(\mathcal{L}(\mathbf{h}, D, \bar{p}, \varphi)) &= \int_{t_0}^T \{\varphi^T \mathbb{J} (\dot{\eta} + \text{ad}_\varphi \eta) - \eta^T Z(\mathbf{h}, D, \bar{p})\} dt \\ &= \int_{t_0}^T \eta^T (\text{ad}_\varphi^* \mathbb{J} \varphi - Z(\mathbf{h}, D, \bar{p}) - \mathbb{J} \dot{\varphi}) dt + \varphi^T \mathbb{J} \eta|_{t_0}^T \\ &= \int_{t_0}^T \eta^T (\text{ad}_\varphi^* \mathbb{J} \varphi - Z(\mathbf{h}, D, \bar{p}) - \mathbb{J} \dot{\varphi}) dt, \end{aligned} \quad (45)$$

applying fixed endpoint variations with  $\eta(t_0) = \eta(T) = 0$ . Substituting (45) in expression (37) one obtains

$$\mathbb{J} \dot{\varphi} = \text{ad}_\varphi^* \mathbb{J} \varphi - Z(\mathbf{h}, D, \bar{p}) - \mathbb{D} \varphi, \quad (46)$$

where  $Z(\mathbf{h}, D, \bar{p})$  is defined by (43). In order to implement this estimator using the aforementioned measurements, substitute  $Q^T D = \hat{R} L^m$ . This changes the rotational potential energy formed by the estimation errors in attitude (21) to (14). Equation (40) is also reformulated as

$$\begin{aligned} S_K(Q) &= \text{vex}(D W D^T Q - Q^T D W D^T) \\ &= \text{vex}(D W (L^m)^T \hat{R}^T - \hat{R} (L^m) W D^T) = S_\Gamma(\hat{R}). \end{aligned} \quad (47)$$

Finally, the second row in the matrix  $Z(\mathbf{h}, D, \bar{p})$  is replaced by

$$\begin{aligned} \kappa\{Q^T x + (I - Q^T)\bar{p}\} &= \kappa\{Q^T b - \hat{b} + \bar{p} - Q^T \bar{p}\} \\ &= \kappa\{\hat{R}R^T(b - \bar{p}) - \hat{b} + \bar{p}\} \\ &= \kappa\{-\hat{R}\bar{a}^m - \hat{b} + \bar{p}\}. \end{aligned} \quad (48)$$

Taking these changes into account, one could obtain the first of equations (32) with  $Z(\hat{\mathbf{g}}, L^m, D, \bar{a}^m, \bar{p})$  and  $S_\Gamma(\hat{R})$  defined by (33) and (34), respectively. Thus, the complete nonlinear estimator equations are given by (32).  $\square$

This is a fundamentally new idea of applying a principle from variational mechanics to obtain a state estimator, recently applied to rigid body attitude estimation in [10]. This approach differs from the “minimum-energy” approach to nonlinear estimation due to Mortensen [26] in some important ways. The minimum-energy approach applies Hamilton-Jacobi-Bellman (HJB) theory [16], which can only be “approximately solved.” This approach was recently applied to state estimation of rigid body attitude motion in [39]. This HJB formulation can only be approximately solved in practice, using a Riccati-like equation, to obtain a near-optimal filter that has no guarantees on stability. In the proposed approach, the time evolution of  $(\hat{\mathbf{g}}, \hat{\xi})$  has the form of the dynamics of a rigid body with Rayleigh dissipation. This results in an estimator for the motion states  $(\mathbf{g}, \xi)$  that dissipates the “energy” content in the estimation errors  $(\mathbf{h}, \varphi) = (\mathbf{g}\hat{\mathbf{g}}^{-1}, \text{Ad}_{\hat{\mathbf{g}}}(\xi - \hat{\xi}))$  to provide guaranteed asymptotic stability in the case of perfect measurements [10]. The differences between these two approaches were detailed in [9], for rigid body attitude estimation.

The proposed estimator combines certain desirable features of stochastic estimation and observer design approaches to state estimation for unmanned vehicles, when simultaneous inertial vector measurements and optical measurements of fixed beacons or landmarks are available. This nonlinear estimator is robust to measurement noise and does not require a dynamics model for the vehicle; instead, it estimates the dynamics of the vehicle given the measurement model in Section 2. The variational pose estimator can also be interpreted as a low-pass stable filter (cf. [35]). Indeed, one can connect the low-pass filter interpretation to the simple example of the natural dynamics of a mass-spring-damper system. This is a consequence of the fact that the mass-spring-damper system is a mechanical system with passive dissipation, evolving on a configuration space that is the vector space of real numbers,  $\mathbb{R}$ . In fact, the equation of motion of this system can be obtained by application of the Lagrange-d’Alembert principle on the configuration space  $\mathbb{R}$ . If this analogy or interpretation is extended to a system evolving on a Lie group as a configuration space, then the generalization of the

mass-spring-damper system is a “forced Euler-Poincaré system” [5, 21] with passive dissipation, as is obtained here. Explicit expressions for the vector of velocities  $\xi^m$  can be obtained for two common cases when these velocities are not directly measured. These two cases are dealt with in the next subsection.

### 3.3 Variational Estimator Implemented without Direct Velocity Measurements

The velocity measurements in (32) can be replaced by filtered velocity estimates obtained by linear filtering of optical and inertial measurements using, e.g., a second-order Butterworth filter. This is both useful and necessary when velocities are not directly measured. The filtered values  $\xi^f$  are then used in place of  $\xi^m$  to enhance the nonlinear estimator given by Theorem 3.3. Denote the measured vector quantity at time  $t$  by  $z^m$ . A linear second-order filter of the form:

$$\ddot{z}^f + 2\mu\omega_n\dot{z}^f = \omega_n^2(z^m - z^f), \quad (49)$$

is used, where  $\omega_n$  is the natural (cutoff) frequency,  $\mu$  is the damping ratio, and  $z^f$  is the filtered value of  $z^m$ . Thereafter,  $z^f$  is used in place of  $z^m$  in equations (32).

#### 3.3.1 Angular velocity is measured using rate gyros

For the case that rate gyro measurements of angular velocities are available besides the  $j$  feature point (or beacon) position measurements, the linear velocities of the rigid body can be calculated using each single position measurement by rewriting (52) as

$$\nu^f = (a_j^f)^\times \Omega^f - v_j^f, \quad (50)$$

for the  $j^{\text{th}}$  point. Averaging the values of  $\nu$  derived from all feature points gives a more reliable result. Therefore, the rigid body’s filtered velocities are expressed in this case as

$$\xi^f = \begin{bmatrix} \Omega^f \\ \frac{1}{j} \sum_{j=1}^j (a_j^f)^\times \Omega^f - v_j^f \end{bmatrix}. \quad (51)$$

#### 3.3.2 Translational and angular velocity measurements are not available

In the case that both angular and translational velocity measurements are not available or accurate, rigid body velocities can be calculated in terms of the inertial and optical measurements. In order to do so, one can differ-

entiate (2) as follows

$$\begin{aligned} \dot{p}_j &= R\Omega^\times a_j + R\dot{a}_j + \dot{b} = R(\Omega^\times a_j + \dot{a}_j + \nu) = 0 \\ \Rightarrow \dot{a}_j - a_j^\times \Omega + \nu &= 0 \\ \Rightarrow v_j = \dot{a}_j &= [a_j^\times \quad -I]\xi = G(a_j)\xi, \end{aligned} \quad (52)$$

where  $G(a_j) = [a_j^\times \quad -I]$  has full row rank. From vision-based or Doppler lidar sensors, one can also measure the velocities of the observed points in frame  $\mathcal{S}$ , denoted  $v_j^m$ . Here, velocity measurements as would be obtained from vision-based sensors is considered. The measurement model for the velocity is of the form

$$v_j^m = G(a_j)\xi + \vartheta_j, \quad (53)$$

where  $\vartheta_j \in \mathbb{R}^3$  is the additive error in velocity measurement  $v_j^m$ . Instantaneous angular and translational velocity determination from such measurements is treated in [29]. Note that  $v_j = \dot{a}_j$ , for  $j \in \mathcal{I}(t)$ . As this kinematics indicates, the relative velocities of at least three beacons are needed to determine the vehicle's translational and angular velocities uniquely at each instant. However, when only one or two landmarks/beacons are measured, the estimator can propagate velocity estimates based on a least squares velocity determined from the available measurements. The rigid body velocities in both cases are obtained using the pseudo-inverse of  $\mathbb{G}(A^f)$ :

$$\mathbb{G}(A^f)\xi^f = \mathbb{V}(V^f) \Rightarrow \xi^f = \mathbb{G}^\ddagger(A^f)\mathbb{V}(V^f), \quad (54)$$

$$\text{where } \mathbb{G}(A^f) = \begin{bmatrix} G(a_1^f) \\ \vdots \\ G(a_j^f) \end{bmatrix} \text{ and } \mathbb{V}(V^f) = \begin{bmatrix} v_1^f \\ \vdots \\ v_j^f \end{bmatrix}, \quad (55)$$

for  $1, \dots, j \in \mathcal{I}(t)$ . When at least three beacons are measured,  $\mathbb{G}(A^f)$  is a full column rank matrix, and  $\mathbb{G}^\ddagger(A^f) = \left(\mathbb{G}^\top(A^f)\mathbb{G}(A^f)\right)^{-1}\mathbb{G}^\top(A^f)$  gives its pseudo-inverse. For the case that only one or two beacons are observed,  $\mathbb{G}(A^f)$  is a full row rank matrix, whose pseudo-inverse is given by  $\mathbb{G}^\ddagger(A^f) = \mathbb{G}^\top(A^f)\left(\mathbb{G}(A^f)\mathbb{G}^\top(A^f)\right)^{-1}$ .

#### 4 Stability and Robustness of Estimator

The stability of the estimator (filter) given by Theorem 3.3 is analyzed here. The following result shows that this scheme is stable, with almost global convergence of the estimated states to the real states in the absence of measurement noise.

**Theorem 4.1** *Let the observed position vectors from optical measurements be bounded. Then, the estimator presented in Theorem 3.3 is asymptotically stable at the estimation error state  $(\mathbf{h}, \varphi) = (I, 0)$  in the absence of*

*measurement noise. Further, the domain of attraction of  $(\mathbf{h}, \varphi) = (I, 0)$  is a dense open subset of  $\text{SE}(3) \times \mathbb{R}^6$ .*

*Proof:* In the absence of measurement noise,  $\hat{R}E = Q^\top D$ . Therefore,  $\Phi(\mathcal{U}_r^0(\hat{\mathbf{g}}, L^m, D)) = \Phi(\mathcal{U}_r^0(\mathbf{h}, D))$  is a Morse function on  $\text{SO}(3)$ . The stability of this estimator can be shown using the following candidate Morse-Lyapunov function, which can be interpreted as the total energy function (equal in value to the Hamiltonian) corresponding to the Lagrangian (18):

$$\begin{aligned} V(\mathbf{h}, D, \bar{p}, \varphi) &= \mathcal{T}(\varphi) + \mathcal{U}(\mathbf{h}, D, \bar{p}) \\ &= \frac{1}{2}\varphi^\top \mathbb{J}\varphi + \Phi(\langle I - Q, K \rangle) + \frac{1}{2}\kappa y^\top y. \end{aligned} \quad (56)$$

Note that  $V(\mathbf{h}, D, \bar{p}, \varphi) \geq 0$  and  $V(\mathbf{h}, D, \bar{p}, \varphi) = 0$  if and only if  $(\mathbf{h}, \varphi) = (I, 0)$ . Therefore,  $V(\mathbf{h}, D, \bar{p}, \varphi)$  is positive definite on  $\text{SE}(3) \times \mathbb{R}^6$ . Using (12), one can derive the time derivative of (24) as

$$\begin{aligned} \frac{d}{dt}\mathcal{U}(\mathbf{h}, D, \bar{p}) &= \Phi'(\mathcal{U}_r^0(\mathbf{h}, D))\langle -Q\omega^\times, K \rangle + \kappa(\dot{x} + \dot{Q}\bar{p})^\top(Qy) \\ &= \Phi'(\mathcal{U}_r^0(\mathbf{h}, D))\langle \omega^\times, -Q^\top K \rangle \\ &\quad + \kappa(Qv + Q\omega^\times \bar{p})^\top(Qy) \\ &= \frac{1}{2}\Phi'(\mathcal{U}_r^0(\mathbf{h}, D))\langle \omega^\times, KQ - Q^\top K \rangle \\ &\quad + \kappa(v + \omega^\times \bar{p})^\top y \\ &= \Phi'(\mathcal{U}_r^0(\mathbf{h}, D))S_K^\top(Q)\omega + \kappa y^\top v + \kappa(\bar{p}^\times y)^\top \omega \\ &= Z^\top(\mathbf{h}, D, \bar{p})\varphi, \end{aligned} \quad (57)$$

where  $S_K(Q)$  is defined as (40) and  $Z(\mathbf{h}, D, \bar{p})$  as (43). Therefore, the time derivative of the candidate Morse-Lyapunov function is

$$\begin{aligned} \dot{V}(\mathbf{h}, D, \bar{p}, \varphi) &= \varphi^\top \mathbb{J}\dot{\varphi} + \varphi^\top Z(\mathbf{h}, D, \bar{p}) \\ &= \varphi^\top \left( \text{ad}_\varphi^* \mathbb{J}\varphi - Z(\mathbf{h}, D, \bar{p}) - \mathbb{D}\varphi + Z(\mathbf{h}, D, \bar{p}) \right) \\ &= -\varphi^\top \mathbb{D}\varphi. \end{aligned} \quad (58)$$

noting that  $\varphi^\top \text{ad}_\varphi^* \mathbb{J}\varphi = 0$ . Hence, the derivative of the Morse-Lyapunov function is negative semi-definite. Note that the error dynamics for the pose estimate error  $\mathbf{h}$  is given by (11), while the error dynamics for the velocities estimate error  $\varphi$  is given by (46). Note that  $D(t)$ , as a function of time, is piecewise continuous and uniformly bounded. The first property (piecewise continuity) is naturally satisfied by  $D(t)$ , which is piecewise constant as the number and inertial positions of beacons (or feature points) observed by body-fixed optical sensors is piecewise continuous in time. The second property (uniform boundedness) is satisfied by  $D(t)$  if the position vectors observed are bounded in  $\mathbb{R}^3$ , as assumed in the statement. Therefore, the error dynamics for  $(\mathbf{h}, \varphi)$  is non-autonomous. Considering (56) and (58), and applying



Theorem 8.4 in [13], one can conclude that  $\varphi^T \mathbb{D}\varphi \rightarrow 0$  as  $t \rightarrow \infty$ , which consequently implies  $\varphi \rightarrow 0$ . Thus, the positive limit set for this system is contained in

$$\mathcal{E} = \dot{V}^{-1}(0) = \{(\mathbf{h}, \varphi) \in \text{SE}(3) \times \mathfrak{se}(3) : \varphi \equiv 0\}. \quad (59)$$

Substituting  $\varphi \equiv 0$  in the first equation of the estimator (32), we obtain the positive limit set where  $\dot{V} \equiv 0$  ( $\varphi \equiv 0$ ) as the set

$$\begin{aligned} \mathcal{I} &= \{(\mathbf{h}, \varphi) \in \text{SE}(3) \times \mathbb{R}^6 : Z(\mathbf{h}, D, \bar{p}) \equiv 0, \varphi \equiv 0\} \\ &= \{(\mathbf{h}, \varphi) \in \text{SE}(3) \times \mathbb{R}^6 : Q \in C_Q, Q^T x = 0, \varphi \equiv 0\}, \end{aligned} \quad (60)$$

where  $C_Q$  is defined by (31). Therefore, in the absence of measurement errors, all the solutions of this estimator converge asymptotically to the set  $\mathcal{I}$ . Define  $\mathcal{U}_r(Q) := \Phi((I - Q, K))$ , which is the attitude measurement residual in the case of perfect measurements. Thus, the attitude estimate error converges to the set of critical points of  $\mathcal{U}_r(Q)$  in this intersection, and the position estimate error  $x$  converges to zero. The unique global minimum of  $\mathcal{U}_r(Q)$  is at  $Q = I$  (Lemma 2.1 in [10]), so this estimation error is asymptotically stable.

Now consider the set

$$\mathcal{C} = \mathcal{I} \setminus (I, 0), \quad (61)$$

which consists of all stationary states that the estimation errors may converge to, besides the desired estimation error state  $(I, 0)$ . Note that all states in the stable manifold of a stationary state in  $\mathcal{C}$  converge to this stationary state. From the properties of the critical points  $Q_\iota \in C_Q \setminus (I)$  of  $\mathcal{U}_r^0(Q)$ , ( $\iota = 1, 2, 3$ ) given in Lemma 2.1 of [10], we see that the stationary points in

$$\mathcal{I} \setminus (I, 0) = \left\{ \left( \begin{bmatrix} Q_\iota & 0 \\ 0 & 1 \end{bmatrix}, 0 \right) : Q_\iota \in C_Q \setminus (I) \right\}$$

have stable manifolds whose dimensions depend on the index of  $Q_\iota$ . Since the velocities estimate error  $\varphi$  converges globally to the zero vector, the dimension of the stable manifold

$\mathcal{M}_\iota^S$  of the critical points, i.e.  $\left( \begin{bmatrix} Q_\iota & 0 \\ 0 & 1 \end{bmatrix}, 0 \right) \in \text{SE}(3) \times \mathbb{R}^6$  is

$$\dim(\mathcal{M}_\iota^S) = 9 + (3 - \text{index of } Q_\iota) = 12 - \text{index of } Q_\iota. \quad (62)$$

Therefore, the stable manifolds of  $(\mathbf{h}, \varphi) = \left( \begin{bmatrix} Q_\iota & 0 \\ 0 & 1 \end{bmatrix}, 0 \right)$

are nine-dimensional, ten-dimensional, or eleven-dimensional, depending on the index of  $Q_\iota \in C_Q \setminus (I)$  according to (62). Moreover, the value of the Lyapunov function  $V(\mathbf{h}, D, \varphi)$  is non-decreasing (increasing when  $(\mathbf{h}, \varphi) \notin \mathcal{I}$ ) for trajectories on these manifolds when

going backwards in time. This implies that the metric distance between error states  $(\mathbf{h}, \varphi)$  along these trajectories on the stable manifolds  $\mathcal{M}_\iota^S$  grows with the time separation between these states, and this property does not depend on the choice of the metric on  $\text{SE}(3) \times \mathbb{R}^6$ . Therefore, these stable manifolds are embedded (closed) submanifolds of  $\text{SE}(3) \times \mathbb{R}^6$  and so is their union. Clearly, all states starting in the complement of this union, converge to the stable equilibrium  $\left( \begin{bmatrix} Q_\iota & 0 \\ 0 & 1 \end{bmatrix}, 0 \right) = (I, 0)$ ;

therefore the domain of attraction of this equilibrium is

$$\text{DOA}\{(I, 0)\} = \text{SE}(3) \times \mathbb{R}^6 \setminus \left\{ \cup_{\iota=1}^3 \mathcal{M}_\iota^S \right\},$$

which is a dense open subset of  $\text{SE}(3) \times \mathbb{R}^6$ .  $\square$

Therefore, the domain of attraction for the variational estimation scheme at  $(\mathbf{h}, \varphi) = (I, 0)$  is almost global over the state space  $\text{TSE}(3) \simeq \text{SE}(3) \times \mathbb{R}^6$ , which is the best possible with continuous control and navigation schemes for systems evolving on a non-contractible state space [7, 24]. In the presence of measurement noise with bounded frequencies and amplitudes, one can show that the expected values of the state estimates converge to a bounded neighborhood of the true states. The size of this neighborhood, which can be considered as a measure of the robustness of this estimation scheme, depends on the values of the estimator gains  $\mathbb{J}$ ,  $W$  and  $\mathbb{D}$ . These estimator gains can be selected based on balancing the transient and steady-state behavior of the estimator.

**Remark 4.2** *In the special case that the weight matrix  $W$  in Wahba's function is chosen as a piecewise time constant matrix according to Lemma 3.2,  $K = DWD^T$  is a constant matrix for all time. Therefore, the RHS of (46) is not explicitly dependent on time. This makes  $(\mathbf{h}, \varphi)$  an autonomous system and therefore the use of Theorem 8.4 of [13] is not required to prove asymptotic stability. One can apply LaSalle's invariance principle (Theorem 4.4 in [13]) to prove the convergence of state estimates to the equilibrium  $(I, 0)$  in this case.*

## 5 Discretization for Computer Implementation

For onboard computer implementation, the variational estimation scheme outlined above has to be discretized. This discretization is carried out in the framework of discrete geometric mechanics, and the resulting discrete-time estimator is in the form of a Lie group variational integrator (LGVI), as in [30]. Since the estimation scheme proposed here is obtained from a variational principle of mechanics, it can be discretized by applying the discrete Lagrange-d'Alembert principle [22]. Consider an interval of time  $[t_0, T] \in \mathbb{R}^+$  separated into  $N$  equal-length subintervals  $[t_i, t_{i+1}]$  for  $i = 0, 1, \dots, N$ , with  $t_N = T$  and  $t_{i+1} - t_i = \Delta t$  is the time step size. Let  $(\hat{\mathbf{g}}_i, \hat{\xi}_i) \in \text{SE}(3) \times \mathbb{R}^6$  denote the discrete state estimate at time  $t_i$ , such that  $(\hat{\mathbf{g}}_i, \hat{\xi}_i) \approx (\hat{\mathbf{g}}(t_i), \hat{\xi}(t_i))$  where

$(\hat{\mathbf{g}}(t), \hat{\xi}(t))$  is the exact solution of the continuous-time estimator at time  $t \in [t_0, T]$ . Let the values of the discrete-time measurements  $\xi^m$ ,  $\bar{a}^m$  and  $L^m$  at time  $t_i$  be denoted as  $\xi_i^m$ ,  $\bar{a}_i^m$  and  $L_i^m$ , respectively. Further, denote the corresponding values for the latter two quantities in inertial frame at time  $t_i$  by  $\bar{p}_i$  and  $D_i$ , respectively. The term representing the energy content of the pose estimation error, given by (16), is discretized as

$$\begin{aligned} \mathcal{U}(\hat{\mathbf{g}}_i, L_i^m, D_i, \bar{a}_i^m, \bar{p}_i) &= \mathcal{U}_r(\hat{\mathbf{g}}_i, L_i^m, D_i) + \mathcal{U}_t(\hat{\mathbf{g}}_i, \bar{a}_i^m, \bar{p}_i) \\ &= \Phi(\mathcal{U}_r^0(\hat{\mathbf{g}}_i, L_i^m, D_i)) + \mathcal{U}_t(\hat{\mathbf{g}}_i, \bar{a}_i^m, \bar{p}_i) \\ &= \Phi\left(\frac{1}{2}\langle D_i - \hat{R}_i L_i^m, (D_i - \hat{R}_i L_i^m) W_i \rangle\right) \\ &\quad + \frac{1}{2} \kappa \|\bar{p}_i - \hat{R}_i \bar{a}_i^m - \hat{b}_i\|^2, \end{aligned} \quad (63)$$

where  $W_i$  is the matrix of weight factors corresponding to  $D_i$  at time  $t_i$ . The term encapsulating the energy in the velocities estimate error (17), is discretized as

$$\mathcal{T}(\varphi(\hat{\mathbf{g}}_i, \xi_i^m, \hat{\xi}_i)) = \frac{1}{2} \varphi(\hat{\mathbf{g}}_i, \xi_i^m, \hat{\xi}_i)^T \mathbb{J} \varphi(\hat{\mathbf{g}}_i, \xi_i^m, \hat{\xi}_i), \quad (64)$$

where  $\mathbb{J} = \text{diag}(J, M)$  and  $M, J$  are positive definite matrices.

**Lemma 5.1** *In the absence of measurement noise, the discrete-time Lagrangian is of the form*

$$\begin{aligned} \mathcal{L}(\mathbf{h}_i, D_i, \bar{p}_i, \varphi_i) &= \frac{1}{2} \langle \mathcal{J} \omega_i^\times, \omega_i^\times \rangle + \frac{1}{2} \langle M v_i, v_i \rangle \\ &\quad - \Phi(\langle I - Q_i, K_i \rangle) - \frac{1}{2} \kappa y_i^T y_i, \end{aligned} \quad (65)$$

where  $y_i \equiv y(\mathbf{h}_i, \bar{p}_i) = Q_i^T x_i + (I - Q_i^T) \bar{p}_i$  and  $\mathcal{J}$  is defined in terms of the matrix  $J$  by  $\mathcal{J} = \frac{1}{2} \text{trace}[J] I - J$ .

A Lie group variational integrator (LGVI) introduced in [32] is applied to the discrete-time Lagrangian (65) to obtain the discrete-time filter.

**Theorem 5.2** *A first-order discretization of the estimator proposed in Theorem 3.3 is given by*

$$(J \omega_i)^\times = \frac{1}{\Delta t} (F_i \mathcal{J} - \mathcal{J} F_i^T), \quad (66)$$

$$\begin{aligned} (M + \Delta t \mathbb{D}_t) v_{i+1} &= F_i^T M v_i \\ &\quad + \Delta t \kappa (\hat{b}_{i+1} + \hat{R}_{i+1} \bar{a}_{i+1}^m - \bar{p}_{i+1}), \end{aligned} \quad (67)$$

$$\begin{aligned} (J + \Delta t \mathbb{D}_r) \omega_{i+1} &= F_i^T J \omega_i + \Delta t M v_{i+1} \times v_{i+1} \\ &\quad + \Delta t \kappa \bar{p}_{i+1}^\times (\hat{b}_{i+1} + \hat{R}_{i+1} \bar{a}_{i+1}^m) \end{aligned} \quad (68)$$

$$\begin{aligned} -\Delta t \Phi'(\mathcal{U}_r^0(\hat{\mathbf{g}}_{i+1}, L_{i+1}^m, D_{i+1})) S_{\Gamma_{i+1}}(\hat{R}_{i+1}), \\ \hat{\xi}_i = \xi_i^m - \text{Ad}_{\hat{\mathbf{g}}_i^{-1}} \varphi_i, \end{aligned} \quad (69)$$

$$\hat{\mathbf{g}}_{i+1} = \hat{\mathbf{g}}_i \exp(\Delta t \hat{\xi}_i^\vee), \quad (70)$$

where  $F_i \in \text{SO}(3)$ ,  $(\hat{\mathbf{g}}(t_0), \hat{\xi}(t_0)) = (\hat{\mathbf{g}}_0, \hat{\xi}_0)$ ,  $\varphi_i = [\omega_i^T v_i^T]^T$ , and  $S_{\Gamma_i}(\hat{R}_i)$  is the value of  $S_\Gamma(\hat{R})$  at time  $t_i$ , with  $S_\Gamma(\hat{R})$  as defined by (34).

*Proof:* Consider first variations with fixed endpoints for the pose estimation errors in discrete time given by:

$$\delta Q_i = Q_i \Sigma_i^\times, \quad \Sigma_0 = \Sigma_N = 0, \quad (71)$$

$$\delta x_i = Q_i \rho_i, \quad \rho_0 = \rho_N = 0, \quad (72)$$

where  $\Sigma_i, \rho_i \in \mathbb{R}^3$  are ‘‘discrete variation vectors’’. It can be shown that for any  $\omega \in \mathbb{R}^3$  we have

$$(J \omega)^\times = \omega^\times \mathcal{J} + \mathcal{J} \omega^\times. \quad (73)$$

Discretizing (12) assuming that the angular velocity estimation error is constant in the time interval  $[t_i, t_{i+1}]$  with a constant time step size  $\Delta t$ , one gets

$$Q_{i+1} = Q_i F_i, \quad i \in \{0, 1, 2, \dots, N-1\}, \quad (74)$$

where  $F_i \in \text{SO}(3)$  is given by

$$F_i = \exp(\Delta t \omega_i^\times) \approx I + \Delta t \omega_i^\times. \quad (75)$$

The variation of  $F_i$  can be derived from (74) and  $\delta Q_i = Q_i \Sigma_i^\times$ . Thus

$$\delta F_i = -\Sigma_i^\times F_i + F_i \Sigma_{i+1}^\times. \quad (76)$$

Using (73) and (75), one can enforce the skew-symmetry of  $(J \omega_i)^\times$  by

$$\begin{aligned} (J \omega_i)^\times &= \omega_i^\times \mathcal{J} + \mathcal{J} \omega_i^\times \approx \frac{1}{\Delta t} \left( (F_i - I) \mathcal{J} - \mathcal{J} (F_i^T - I) \right) \\ &= \frac{1}{\Delta t} (F_i \mathcal{J} - \mathcal{J} F_i^T). \end{aligned} \quad (77)$$

From (11), the continuous rate of change of the attitude estimation error is  $\dot{x} = Q v$ , which can be approximated to first order in discrete-time as

$$\frac{x_{i+1} - x_i}{\Delta t} \approx Q_i v_i \Rightarrow x_{i+1} = \Delta t Q_i v_i + x_i. \quad (78)$$

The first variation in  $v_i$  is then calculated using (78) as

$$\begin{aligned} \delta v_i &= \delta \left( \frac{1}{\Delta t} Q_i^T (x_{i+1} - x_i) \right) \\ &= -\Sigma_i^\times v_i + \frac{1}{\Delta t} Q_i^T (\delta x_{i+1} - \delta x_i) \\ &= -\Sigma_i^\times v_i + \frac{1}{\Delta t} F_i \rho_{i+1} - \frac{1}{\Delta t} \rho_i. \end{aligned} \quad (79)$$

The discrete Lagrangian (65) can be rewritten as

$$\begin{aligned} \mathcal{L}(\mathbf{h}_i, D_i, \bar{p}_i, F_i, v_i) &= \frac{1}{2\Delta t} \langle \mathcal{J}(F_i - I), (F_i - I) \rangle \\ &+ \frac{\Delta t}{2} \langle Mv_i, v_i \rangle - \Delta t \Phi(\mathcal{U}_r^0(\mathbf{h}_i, D_i)) \\ &- \frac{\Delta t}{2} \kappa(Q_i y_i)^\top (Q_i y_i). \end{aligned} \quad (80)$$

The action functional (19) is replaced by the action sum

$$\mathcal{S}_d(\mathcal{L}(\mathbf{h}_i, D_i, \bar{p}_i, F_i, v_i)) = \Delta t \sum_{i=0}^{N-1} \mathcal{L}(\mathbf{h}_i, D_i, \bar{p}_i, F_i, v_i). \quad (81)$$

Applying the discrete Lagrange-d'Alembert principle with two Rayleigh dissipation terms for angular and translational motions gives

$$\begin{aligned} \delta \mathcal{S}_d(\mathcal{L}(\mathbf{h}_i, D_i, \bar{p}_i, F_i, v_i)) &+ \Delta t \sum_{i=0}^{N-1} \left\{ \langle \Sigma_i, \tau_i \rangle + \langle \rho_i, f_i \rangle \right\} = 0 \\ \Rightarrow \sum_{i=0}^{N-1} \left\{ \frac{1}{\Delta t} \langle \delta F_i, \mathcal{J}(F_i - I) \rangle + \Delta t \langle \delta v_i, Mv_i \rangle \right. \\ &- \frac{\Delta t}{2} \Phi'(\mathcal{U}_r^0(\mathbf{h}_i, D_i)) \langle \Sigma_i^\times, S_{K_i}^\times(Q_i) \rangle - \Delta t \kappa \langle \rho_i, y_i \rangle \\ &\left. - \Delta t \kappa \langle \Sigma_i^\times, y_i \bar{p}_i^\top \rangle + \frac{\Delta t}{2} \langle \Sigma_i^\times, \tau_i^\times \rangle + \Delta t \langle \rho_i, f_i \rangle \right\} = 0. \end{aligned} \quad (82)$$

As symmetric matrices are orthogonal to skew-symmetric matrices in the trace inner product, using (75) we can rewrite the first term in (80) as

$$\begin{aligned} \langle \delta F_i, \mathcal{J}(F_i - I) \rangle &= \langle \Sigma_i^\times, \mathcal{J}F_i^\top \rangle - \langle \Sigma_{i+1}^\times, F_i^\top \mathcal{J} \rangle \\ &= \frac{1}{2} \langle \Sigma_i^\times, \mathcal{J}F_i^\top \rangle - \frac{1}{2} \langle \Sigma_i^\times, F_i \mathcal{J} \rangle \\ &\quad - \frac{1}{2} \langle \Sigma_{i+1}^\times, F_i^\top \mathcal{J} \rangle + \frac{1}{2} \langle \Sigma_{i+1}^\times, \mathcal{J}F_i \rangle \\ &= -\frac{\Delta t}{2} \langle \Sigma_i^\times, (J\omega_i)^\times \rangle + \frac{\Delta t}{2} \langle \Sigma_{i+1}^\times, F_i^\top (J\omega_i)^\times F_i \rangle. \end{aligned} \quad (83)$$

Hence equation (82) can be re-expressed as

$$\begin{aligned} \sum_{i=0}^{N-1} \left\{ -\frac{1}{2} \langle \Sigma_i^\times, (J\omega_i)^\times \rangle + \frac{1}{2} \langle \Sigma_{i+1}^\times, F_i^\top (J\omega_i)^\times F_i \rangle \right. \\ &- \frac{\Delta t}{2} \langle \Sigma_i^\times, (v_i \times Mv_i)^\times \rangle + \langle F_i \rho_{i+1}, Mv_i \rangle \\ &- \langle \rho_i, Mv_i \rangle - \frac{\Delta t}{2} \Phi'(\mathcal{U}_r^0(\mathbf{h}_i, D_i)) \langle \Sigma_i^\times, S_{K_i}^\times(Q_i) \rangle \\ &- \kappa \Delta t \langle \rho_i, y_i \rangle - \frac{\kappa \Delta t}{2} \langle \Sigma_i^\times, (\bar{p}_i^\times y_i)^\times \rangle \\ &\left. + \frac{\Delta t}{2} \langle \Sigma_i^\times, \tau_i^\times \rangle + \Delta t \langle \rho_i, f_i \rangle \right\} = 0. \end{aligned} \quad (84)$$

Separating this equation into two (rotational and translational) parts leads to

$$(M + \Delta t \mathbb{D}_t) v_{i+1} = F_i^\top M v_i - \Delta t \kappa y_{i+1}, \quad (85)$$

$$\begin{aligned} (J + \Delta t \mathbb{D}_r) \omega_{i+1} &= F_i^\top J \omega_i + \Delta t M v_{i+1} \times v_{i+1} \\ &- \Delta t \kappa \bar{p}_{i+1}^\times y_{i+1} \\ &- \Delta t \Phi'(\mathcal{U}_r^0(\mathbf{h}_{i+1}, D_{i+1})) S_{K_{i+1}}(Q_{i+1}), \end{aligned} \quad (86)$$

using the identity  $\mathcal{F}^\top \omega^\times \mathcal{F} = (\mathcal{F}^\top \omega)^\times$  and by replacing  $\tau_i = -\mathbb{D}_r \omega_i$  and  $f_i = -\mathbb{D}_t v_i$ , where  $\mathbb{D}_r$  and  $\mathbb{D}_t$  are positive definite matrices such that

$$\mathbb{D} = \begin{bmatrix} \mathbb{D}_r & 0 \\ 0 & \mathbb{D}_t \end{bmatrix}.$$

In the presence of measurement noise,  $Q_i^\top D_i$  and  $y_i$  are replaced by  $\hat{R}_i L_i^m$  and  $\bar{p}_i - \hat{b}_i - \hat{R}_i \bar{a}_i^m$ , respectively. These give the discrete-time state estimator in the form of the Lie group variational integrator (66)-(70).  $\square$

Model-based discrete-time rigid body state estimators using LGVI schemes for attitude estimation were reported in [30, 31], but dynamics model-free state estimators using LGVIs have appeared only recently in [10, 12].

**Remark 5.3** *In the absence of any direct velocity measurements or only angular velocity measurements, the expressions provided in Section 3.3 to calculate rigid body velocities are still valid in discrete-time. One can use the discrete-time variables introduced in this section in place of their continuous-time counterparts. The second-order Butterworth filter (49) is discretized using the Newmark- $\beta$  Method as follows:*

$$\begin{cases} z_{i+1}^f = z_i^f + \Delta t \dot{z}_i^f + \frac{\Delta t^2}{4} (\ddot{z}_i^f + \ddot{z}_{i+1}^f) \\ \dot{z}_{i+1}^f = \dot{z}_i^f + \frac{\Delta t}{2} (\ddot{z}_i^f + \ddot{z}_{i+1}^f) \end{cases}. \quad (87)$$

Choosing  $\omega_n = 2$  and  $\mu = \frac{1}{2}$ , this method gives the filtered positions and velocities as follows:

$$\begin{aligned} \begin{Bmatrix} z_{i+1}^f \\ \dot{z}_{i+1}^f \end{Bmatrix} &= \frac{1}{4 + 4\mu\omega_n\Delta t + \omega_n^2\Delta t^2} \\ &\begin{bmatrix} 4 + 4\mu\omega_n\Delta t - \omega_n^2\Delta t^2 & 4\Delta t & \omega_n^2\Delta t^2 \\ -4\omega_n^2\Delta t & 4 - 4\mu\omega_n\Delta t - \omega_n^2\Delta t^2 & 2\omega_n^2\Delta t \end{bmatrix} \\ &\begin{Bmatrix} z_i^f \\ \dot{z}_i^f \\ z_i^m + z_{i+1}^m \end{Bmatrix}. \end{aligned} \quad (88)$$

where  $z_i^m$  and  $\dot{z}_i^f$  are the corresponding value of quantities  $z^m$  and  $z^f$  at time instant  $t_i$ , respectively. As with the

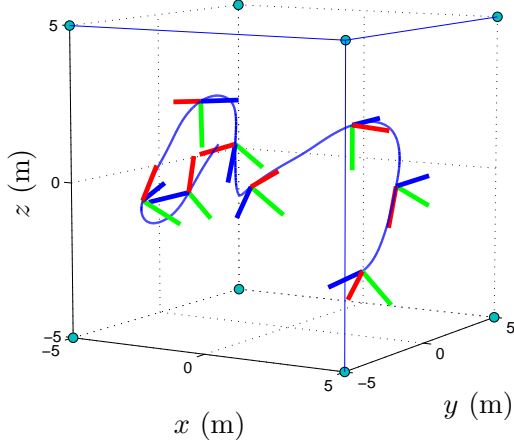


Fig. 2. Position and attitude trajectory of the simulated vehicle in 3D space.

continuous time version,  $\xi_i^m$  can be replaced with  $\xi_i^f$  in the estimator equations.

## 6 Numerical Simulations

This section presents numerical simulation results for the discrete-time estimator obtained in Section 5. In order to numerically simulate this estimator, simulated true states of an aerial vehicle flying in a room are produced using the kinematics and dynamics equations of a rigid body. The vehicle mass and moment of inertia are taken to be  $m_v = 420$  g and  $J_v = [51.2 \ 60.2 \ 59.6]^T$  g.m<sup>2</sup>, respectively. The resultant external forces and torques applied on the vehicle are  $\phi_v(t) = 10^{-3}[10 \cos(0.1t) \ 2 \sin(0.2t) \ -2 \sin(0.5t)]^T$  N and  $\tau_v(t) = 10^{-6}\phi_v(t)$  N.m, respectively. The room is assumed to be a cubic space of size 10m×10m×10m with the inertial frame origin at the center of this cube. The initial attitude and position of the vehicle are:

$$R_0 = \expm_{\text{SO}(3)} \left( \left( \frac{\pi}{4} \times \begin{bmatrix} 3 \\ 7 \\ -\frac{6}{7} \frac{2}{7} \end{bmatrix}^T \right)^\times \right),$$

and  $b_0 = [2.5 \ 0.5 \ -3]^T$  m. (89)

This vehicle's initial angular and translational velocity respectively, are:

$$\Omega_0 = [0.2 \ -0.05 \ 0.1]^T \text{ rad/s},$$

and  $\nu_0 = [-0.05 \ 0.15 \ 0.03]^T$  m/s. (90)

The vehicle dynamics is simulated over a time interval of  $T = 150$  s, with a time stepsize of  $\Delta t = 0.02$  s. The trajectory of the vehicle over this time interval is depicted in Fig. 2. The following two inertial directions, corresponding to nadir and Earth's magnetic field direction,

are measured by the inertial sensors on the vehicle:

$$d_1 = [0 \ 0 \ -1]^T, \quad d_2 = [0.1 \ 0.975 \ -0.2]^T. \quad (91)$$

For optical measurements, eight beacons are located at the eight vertices of the cube, labeled 1 to 8. The positions of these beacons are known in the inertial frame and their index (label) and relative positions are measured by optical sensors onboard the vehicle whenever the beacons come into the field of view of the sensors. Three identical cameras (optical sensors) and inertial sensors are assumed to be installed on the vehicle. The cameras are fixed to known positions on the vehicle, on a hypothetical horizontal plane passing through the vehicle, 120° apart from each other, as shown in Fig. 1. All the camera readings contain random zero mean signals whose probability distributions are normalized bump functions with width of 0.001m. The following are selected for the positive definite estimator gain matrices:

$$J = \text{diag}([0.9 \ 0.6 \ 0.3]),$$

$$M = \text{diag}([0.0608 \ 0.0486 \ 0.0365]), \quad (92)$$

$$\mathbb{D}_r = \text{diag}([2.7 \ 2.2 \ 1.5]), \quad \mathbb{D}_t = \text{diag}([0.1 \ 0.12 \ 0.14]).$$

$\Phi(\cdot)$  could be any  $C^2$  function with the properties described in Section 3, but is selected to be  $\Phi(x) = x$  here. The initial state estimates have the following values:

$$\hat{g}_0 = I, \quad \hat{\Omega}_0 = [0.1 \ 0.45 \ 0.05]^T \text{ rad/s}, \quad (93)$$

and  $\hat{\nu}_0 = [2.05 \ 0.64 \ 1.29]^T$  m/s.

The performance of the proposed estimator is presented for two different cases.

### 6.1 CASE 1: At least three beacons are observed at each time instant

Having three beacons measured at each time instant guarantees full determination of vehicle's translational and angular velocities instantaneously. A conic field of view (FOV) of  $2 \times 40^\circ$  for cameras can satisfy this condition. The vehicle's velocity is calculated by (54) in this case. The discrete-time estimator (66)-(70) is simulated over a time interval of  $T = 20$  s with sampling interval  $\Delta t = 0.02$  s. At each time instant, (66) is solved using the Newton-Raphson iterative method to find an approximation for  $F_i$ . Following this, the remaining equations (all explicit) are solved to generate the estimated states. The principal angle of the attitude estimation error and the position estimation error for CASE 1 are plotted in Fig. 3. Plots of the angular and translational velocity estimation errors are shown in Fig. 4.

### 6.2 CASE 2: Less than three beacons are measured at some time instants

To implement the variational estimator for the case that less than three optical measurements are available,

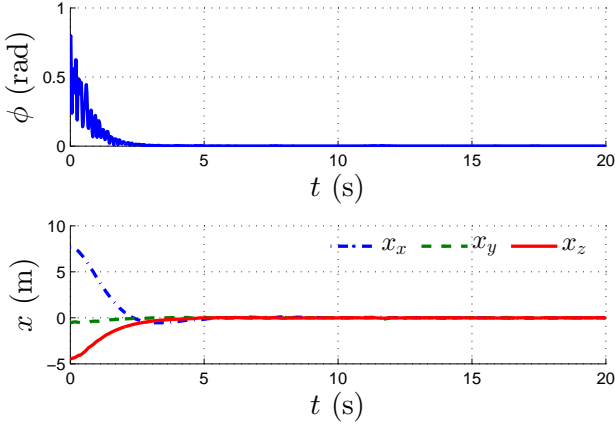


Fig. 3. Principal angle of the attitude and position estimation error for CASE 1.

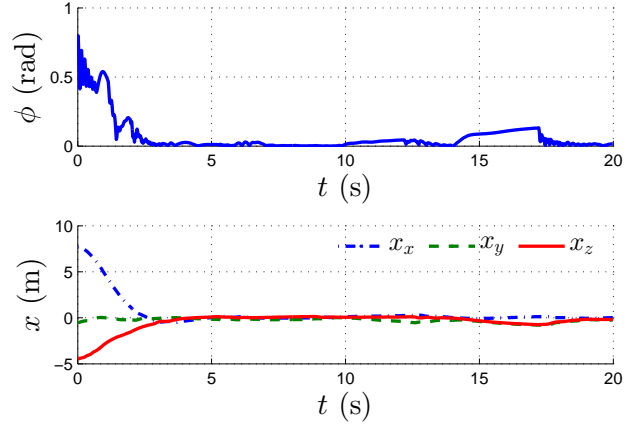


Fig. 5. Principal angle of the attitude and position estimation error for CASE 2.

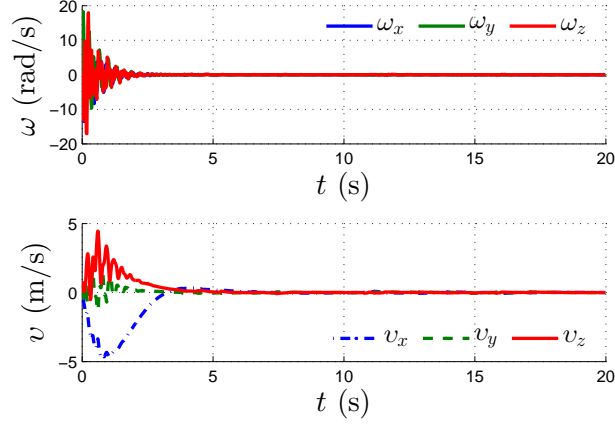


Fig. 4. Angular and translational velocity estimation error for CASE 1.

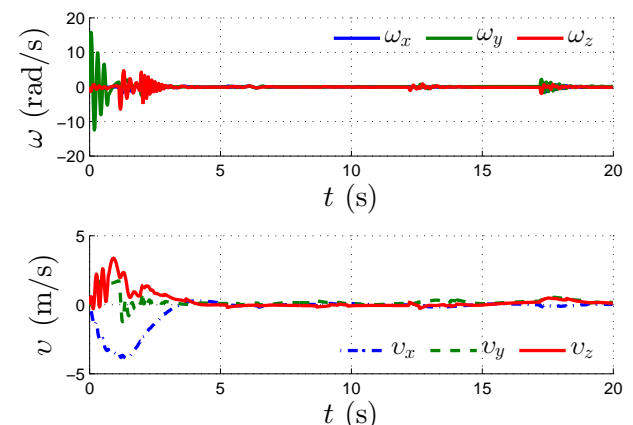


Fig. 6. Angular and translational velocity estimation error for CASE 2.

the field of view of the cameras is decreased to limit the number of beacons observed. Assuming the cameras have conical fields of view of  $2 \times 25^\circ$ , the minimum number of beacons observed instantaneously drops to 1 during the simulated time interval. The dynamics model for the aerial vehicle, simulated time duration, and sample rate are identical to CASE 1. Fig. 5 depicts the principal angle of the attitude estimation error and the position estimation error for CASE 2, and Fig. 6 shows the angular and translational velocity estimation errors. All estimation errors are shown to converge to a neighborhood of  $(\mathbf{h}, \varphi) = (I, 0)$  in both cases, where the size of this neighborhood depends on the magnitude of measurement noise.

## 7 Conclusion

This article proposes an estimator for rigid body pose and velocities, using optical and inertial measurements by sensors onboard the rigid body. The sensors are assumed to provide measurements in continuous-time or

at a sufficiently high frequency, with bounded measurement noise. An artificial kinetic energy quadratic in rigid body velocity estimate errors is defined, as well as two fictitious potential energies: (1) a generalized Wahba's cost function for attitude estimation error in the form of a Morse function, and (2) a quadratic function of the vehicle's position estimate error. Applying the Lagrange-d'Alembert principle on a Lagrangian consisting of these energy-like terms and a dissipation term linear in velocities estimation error, an estimator is designed on the Lie group of rigid body motions. In the absence of measurement noise, this estimator is shown to be almost globally asymptotically stable, with estimates converging to actual states in a domain of attraction that is open and dense in the state space. The continuous estimator is discretized by applying the discrete Lagrange-d'Alembert principle on the discrete Lagrangian and dissipation terms linear in rotational and translational velocity estimation errors. In the presence of measurement noise, numerical simulations show that state estimates

converge to a bounded neighborhood of the true states. Future extensions of this work include higher-order discretizations of the continuous-time filter given here and obtaining a stochastic interpretation of the variational pose estimator.

## References

- [1] Aguiar, A., & Hespanha, J. (2006). Minimum-energy state estimation for systems with perspective outputs. *IEEE Transactions on Automatic Control*, 51(2), 226–241.
- [2] Amelin, K. S., & Miller, A. B. (2014). An algorithm for refinement of the position of a light UAV on the basis of Kalman filtering of bearing measurements. *Journal of Communications Technology and Electronics*, 59(6), 622–631.
- [3] Bayadi, R., & Banavar, R. N. (2014). Almost global attitude stabilization of a rigid body for both internal and external actuation schemes. *European Journal of Control*, 20(1), 45–54.
- [4] Black, H. (1964). A passive system for determining the attitude of a satellite. *American Institute of Aeronautics and Astronautics*, 2(7), 1350–1351.
- [5] Bloch, A. M. (2003). *Nonholonomic Mechanics and Control*. New York: Springer-Verlag.
- [6] Bonnabel, S., Martin, P., & Rouchon, P. (2009). Nonlinear symmetry-preserving observers on Lie groups. *IEEE Transactions on Automatic Control*, 54(7), 1709–1713.
- [7] Chaturvedi, N. A., Sanyal, A. K., & McClamroch, N. H. (2011). Rigid-body attitude control. *IEEE Control Systems Magazine*, 31(3), 30–51.
- [8] Goodarzi, F., Lee, D., and Lee, T. (2013). Geometric nonlinear PID control of a quadrotor UAV on SE(3). In *Proceedings of the European Control Conference* (pp. 3845–3850). Zurich, Switzerland.
- [9] Izadi, M., Samiei, E., Sanyal, A. K., & Kumar, V. (2015). Comparison of an attitude estimator based on the Lagrange-d’Alembert principle with some state-of-the-art filters. In *Proceedings of the IEEE International Conference on Robotics and Automation* (pp. 2848–2853). Seattle, WA, USA.
- [10] Izadi, M., & Sanyal, A. K. (2014). Rigid body attitude estimation based on the Lagrange-d’Alembert principle. *Automatica*, 50(10), 2570–2577.
- [11] Izadi, M., Sanyal, A. K., Barany, E., & Viswanathan, S. P. (2015). Rigid Body Motion Estimation based on the Lagrange-d’Alembert Principle. In *Proceedings of the 54<sup>th</sup> IEEE Conference on Decision and Control*. Osaka, Japan.
- [12] Izadi, M., Sanyal, A. K., Samiei, E., & Viswanathan, S. P. (2015). Discrete-time rigid body attitude state estimation based on the discrete Lagrange-d’Alembert principle. In *Proceedings of the American Control Conference* (pp. 3392–3397). Chicago, IL, USA.
- [13] Khalil, H. K. (2001). *Nonlinear Systems* (3<sup>rd</sup> edition). Prentice Hall, Upper Saddle River, NJ.
- [14] Khosravian, A., Trunpf, J., Mahony, R., & Hamel, T. (2015). Recursive Attitude Estimation in the Presence of Multi-rate and Multi-delay Vector Measurements. In *Proceedings of the American Control Conference* (pp. 3199–3205). Chicago, IL, USA.
- [15] Khosravian, A., Trunpf, J., Mahony, R., & Lageman, C. (2015). Observers for invariant systems on Lie groups with biased input measurements and homogeneous outputs. *Automatica*, 55, 19–26.
- [16] Kirk, D. E. (1971). *Optimal Control Theory: An Introduction*. Prentice Hall, NY.
- [17] Leishman, R. C., McLain, T. W., & Beard, R. W. (2014). Relative navigation approach for vision-based aerial GPS-denied navigation. *Journal of Intelligent & Robotic Systems*, 74(1-2), 97–111.
- [18] Mahony, R., Hamel, T., & Pfimlin, J. M. (2008). Nonlinear complementary filters on the special orthogonal group. *IEEE Transactions on Automatic Control*, 53(5), 1203–1218.
- [19] Maithripala, D. H., Berg, J. M., & Dayawansa, W. P. (2004). An intrinsic observer for a class of simple mechanical systems on a Lie group. In *Proceedings of the American Control Conference* (pp. 1546–1551). Boston, MA, USA.
- [20] Markley, F. L. (2006). Attitude filtering on SO(3). *The Journal of the Astronautical Sciences*, 54(4), 391–413.
- [21] Marsden, J. E., & Ratiu, T. S. (1999). *Introduction to mechanics and symmetry: a basic exposition of classical mechanical systems* (Vol. 17). Springer Science & Business Media.
- [22] Marsden, J. E., & West, M. (2001). Discrete mechanics and variational integrators. *Acta Numerica*, 10, 357–514.
- [23] Miller, A., & Miller, B. (2014). Tracking of the UAV trajectory on the basis of bearing-only observations. In *Proceedings of the 53rd Annual Conference on Decision and Control* (pp. 4178–4184). Los Angeles, CA, USA.
- [24] Milnor, J. (1963). *Morse Theory*. Princeton University Press, Princeton, NJ.
- [25] Misra, G., Izadi, M., Sanyal, A. K., & Scheeres, D. J. (2015). Coupled orbit-attitude dynamics and relative state estimation of spacecraft near small Solar System bodies. *Advances in Space Research*.
- [26] Mortensen, R. E. (1968). Maximum-likelihood recursive nonlinear filtering. *Journal of Optimization Theory and Applications*, 2(6), 386–394.
- [27] Rehlinger, H., & Ghosh, B. K. (2003). Pose estimation using line-based dynamic vision and inertial sensors. *IEEE Transactions on Automatic Control*, 48(2), 186–199.
- [28] Sanyal, A. K., Fosbury, A., Chaturvedi, N. A., & Bernstein, D. S. (2009). Inertia-free spacecraft attitude tracking with disturbance rejection and almost global stabilization. *Journal of Guidance, Control,*

- and Dynamics*, 32(4), 1167–1178.
- [29] Sanyal, A. K., Izadi, M., & Butcher, E. A. (2014). Determination of relative motion of a space object from simultaneous measurements of range and range rate. In *Proceedings of the American Control Conference* (pp. 1607–1612). Portland, OR, USA.
  - [30] Sanyal, A. K., Lee, T., Leok, M., & McClamroch, N. H. (2008). Global optimal attitude estimation using uncertainty ellipsoids. *Systems & Control Letters*, 57(3), 236–245.
  - [31] Sanyal, A. K., & Nordkvist, N. (2012). Attitude state estimation with multi-rate measurements for almost global attitude feedback tracking. *AIAA Journal of Guidance, Control, and Dynamics*, 35(3), 868–880.
  - [32] Sanyal, A. K., Nordkvist, N., & Chyba, M. (2011). An almost global tracking control scheme for maneuverable autonomous vehicles and its discretization. *IEEE Transactions on Automatic Control*, 56(2), 457–462.
  - [33] Shen, S., Mulgaonkar, Y., Michael, N., & Kumar, V. (2013). Vision-based state estimation and trajectory control towards aggressive flight with a quadrotor. In *Proceedings of the Robotics Science and Systems*.
  - [34] Shen, S., Mulgaonkar, Y., Michael, N., & Kumar, V. (2013). Vision-based state estimation for autonomous rotorcraft MAVs in complex environments. In *Proceedings of the IEEE International Conference on Robotics and Automation* (pp. 1758–1764). Karlsruhe, Germany.
  - [35] Tayebi, A., Roberts, A., & Benallegue, A. (2011). Inertial measurements based dynamic attitude estimation and velocity-free attitude stabilization. In *Proceedings of the American Control Conference* (pp. 1027–1032). San Francisco, CA, USA.
  - [36] Vasconcelos, J. F., Cunha, R., Silvestre, C., & Oliveira, P. (2010). A nonlinear position and attitude observer on SE(3) using landmark measurements. *Systems & Control Letters*, 59, 155–166.
  - [37] Vasconcelos, J. F., Silvestre, C., & Oliveira, P. (2008). A nonlinear GPS/IMU based observer for rigid body attitude and position estimation. In *Proceedings of the IEEE Conference on Decision and Control* (pp. 1255–1260). Cancun, Mexico.
  - [38] Wahba, G. (1965). A least squares estimate of satellite attitude, Problem 65-1. *SIAM Review*, 7(5), 409.
  - [39] Zamani, M. (2013). *Deterministic Attitude and Pose Filtering, an Embedded Lie Groups Approach*. Ph.D. Thesis. Australian National University, Canberra, Australia.
  - [40] Zamani, M., Trumpf, J., & Mahony, R. (2013). Minimum-energy filtering for attitude estimation. *IEEE Transactions on Automatic Control*, 58(11), 2917–2921.